# Individual differences in frontolimbic circuitry and anxiety emerge with adolescent changes in endocannabinoid signaling across species

Dylan G. Gee[a,b,1], Robert N. Fetcho[a,1], Deqiang Jing[b,1], Anfei Li[a,1], Charles E. Glatt[a,b], Andrew T. Drysdale[a], Alexandra O. Cohen[a,b], Danielle V. Dellarco[a,b], Rui R. Yang[b], Anders M. Dale[c,d], Terry L. Jernigan[d], Francis S. Lee[a,b,e,2,3], B.J. Casey[a,b,2,3], and the PING Consortium[4]

[a]Sackler Institute for Developmental Psychobiology, Weill Cornell Medical College of Cornell University, New York, NY 10065; [b]Department of Psychiatry, Weill Cornell Medical College of Cornell University, New York, NY 10065; [c]Departments of Neurosciences, Radiology, and Psychiatry, University of California, San Diego, CA 92093; [d]Department of Cognitive Science, University of California, San Diego, CA 92093; and [e]Department of Pharmacology, Weill Cornell Medical College of Cornell University, New York, NY 10065

Edited by Michael I. Posner, University of Oregon, Eugene, OR, and approved February 17, 2016 (received for review January 2, 2016)

**Anxiety disorders peak in incidence during adolescence, a developmental window that is marked by dynamic changes in gene expression, endocannabinoid signaling, and frontolimbic circuitry. We tested whether genetic alterations in endocannabinoid signaling related to a common polymorphism in fatty acid amide hydrolase (FAAH), which alters endocannabinoid anandamide (AEA) levels, would impact the development of frontolimbic circuitry implicated in anxiety disorders. In a pediatric imaging sample of over 1,000 3- to 21-y-olds, we show effects of the FAAH genotype specific to frontolimbic connectivity that emerge by ∼12 y of age and are paralleled by changes in anxiety-related behavior. Using a knock-in mouse model of the FAAH polymorphism that controls for genetic and environmental backgrounds, we confirm phenotypic differences in frontoamygdala circuitry and anxiety-related behavior by postnatal day 45 (P45), when AEA levels begin to decrease, and also, at P75 but not before. These results, which converge across species and level of analysis, highlight the importance of underlying developmental neurobiology in the emergence of genetic effects on brain circuitry and function. Moreover, the results have important implications for the identification of risk for disease and precise targeting of treatments to the biological state of the developing brain as a function of developmental changes in gene expression and neural circuit maturation.**

FAAH | frontolimbic | gene × development | anxiety | cross-species

Anxiety disorders typically emerge during adolescence, when the incidence of mental illness peaks (1, 2). The developmental phase of adolescence is characterized by dynamic changes in gene expression, frontolimbic circuitry (3, 4), and overall tone of the endocannabinoid system, which are implicated in anxiety (5–7).

The corticolimbic endocannabinoid system undergoes dynamic changes across development. The onset of adolescence is marked by the highest expression of type 1 cannabinoid receptor (CB1) in both cortical and subcortical brain regions, with CB1 expression declining to adult levels throughout adolescence (8, 9). Across the amygdala and prefrontal cortex, fatty acid amide hydrolase (FAAH) expression shows a transient increase from postnatal day 35 (P35) to P45 during adolescence in mice (10). Consistent with the regulatory role of FAAH, anandamide (AEA) levels show an inverse pattern of a peak at P35 and subsequent decrease during adolescence (10, 11). AEA is an endogenous ligand for the CB1 receptor, suggesting that the concurrent changes in AEA and CB1 expression reflect decreasing endocannabinoid signaling during adolescence (12), which may be associated with increasing risk for anxiety (Fig. 1).

A common human polymorphism in the gene encoding FAAH (C385A; rs324420), the primary catabolic enzyme of the prototypical endocannabinoid AEA, regulates FAAH activity. The variant FAAH A385 allele destabilizes the FAAH protein, causing lower levels of FAAH enzymatic activity and/or increased levels of AEA in T lymphocytes and brain (13, 14). Phenotypic expression of common polymorphisms may vary as a function of developmental changes in AEA signaling, gene expression, and neural circuit maturation. Defining the precise interaction of developmental and genetic variation in AEA signaling can advance understanding of the molecular basis of anxiety disorders and facilitate developing FAAH C385A as a biomarker for precise targeting of treatments to the biological state of the developing brain.

To enhance the reliability of human genetic studies of FAAH C385A, we have developed a knock-in mouse that biologically recapitulates the human FAAH A385 allele, displaying reduced FAAH protein levels and enzymatic activity and increased AEA levels in the brain relative to wild-type (WT) mice, which express the ancestral FAAH C385 allele (14). We have shown that the variant FAAH A385 allele is associated with selective enhancement of frontolimbic connectivity implicated in anxiety (15–18) and greater fear extinction in both adult humans and mice (14). In light of the quantitative differences in AEA levels across development and because of the genotype at FAAH C385A, we hypothesized that there would be a gene by development interaction, in which the effects of FAAH C385A on frontolimbic connectivity and anxiety emerge during adolescence.

In this study, we implemented parallel studies in mice and humans across development (19) to determine the developmental

## Significance

Anxiety disorders peak during adolescence, a developmental period that is marked by dynamic changes in gene expression, frontolimbic circuitry, and endocannabinoid signaling. This cross-species study identifies parallel gene by development interactions across humans and a knock-in mouse model of the same fatty acid amide hydrolase (FAAH) polymorphism. The impact of FAAH genetic variation on frontolimbic circuitry and anxiety in mice and humans emerges during adolescence as anandamide levels decrease but not before. These findings have important implications for the identification of risk for disease and precise targeting of treatments to the biological state of the developing brain as a function of developmental changes in gene expression and neural circuit maturation.

Author contributions: F.S.L. and B.J.C. designed research; D.J., A.L., D.V.D., R.R.Y., T.L.J., B.J.C., and P.C. performed research; D.G.G., R.N.F., D.J., A.L., C.E.G., A.T.D., A.O.C., R.R.Y., and A.M.D. analyzed data; and D.G.G., R.N.F., C.E.G., F.S.L., and B.J.C. wrote the paper.

The authors declare no conflict of interest.

This article is a PNAS Direct Submission.

[1]D.G.G., R.N.F., D.J., and A.L. contributed equally to this work.

[2]F.S.L. and B.J.C. contributed equally to this work.

[3]To whom correspondence may be addressed. Email: fslee@med.cornell.edu or bjc2002@med.cornell.edu.

[4]A complete list of the PING Consortium can be found in *Supporting Information*.

This article contains supporting information online at www.pnas.org/lookup/suppl/doi:10.1073/pnas.1600013113/-/DCSupplemental.

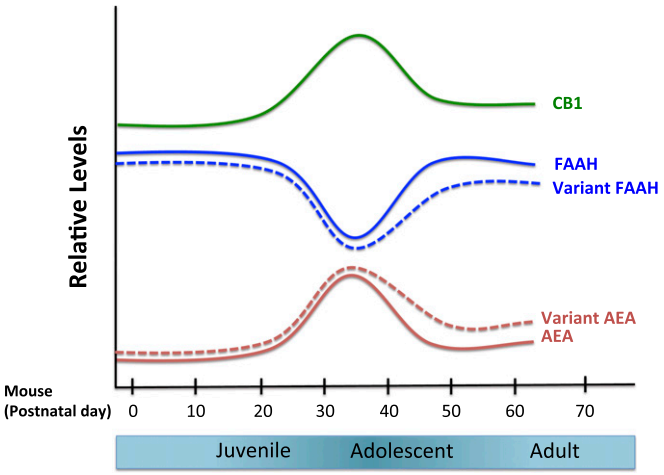


**Fig. 1.** Developmental expression of components of the endocannabinoid system in the brain. Predicted relative concentrations (AEA) and enzymatic activities (FAAH) based on measurement in a rodent system (10). The endocannabinoid system peaks and then wanes in adolescence, which may contribute to changes in risk for anxiety during this developmental stage. FAAH and AEA fluctuate reciprocally across development. Early adolescence is marked by a decrease in FAAH and an increase in AEA levels, whereas FAAH levels increase and AEA levels decrease toward later adolescence (10, 33). CB1 receptor expression peaks with the onset of adolescence (8, 9, 32, 33). The predicted effects of FAAH C385A across development are presented as dotted lines. Adapted from ref. 4, with permission from Elsevier.

course of FAAH C385A effects on frontolimbic circuitry and anxiety-related behavior. Diffusion tensor imaging data from 1,050 human participants ages 3–21 y old (518 females) from the Pediatric Imaging, Neurocognition, and Genetics (PING) Study (20) and tract tracing in FAAH knock-in and WT mice at P23–P75 were used to measure the interaction of FAAH C385A genotype and age on frontolimbic circuitry relative to control tracts. We specifically hypothesized that FAAH A385 allele effects on enhanced frontolimbic circuitry and anxiety would emerge during adolescence, when AEA levels begin to decrease (10, 11), and therefore, may be most sensitive to the additional quantitative effects of the FAAH A385 allele.

## Results

**FAAH C385A-Associated (Phenotypic) Differences in Frontolimbic Circuitry Emerge in Adolescence in Humans and Mice.** Species-specific analyses were performed to assess the effects of FAAH C385A genotype on frontolimbic connectivity across age. In humans, we examined connectivity within the uncinate fasciculus (UF), a white matter tract in the human brain that connects limbic structures in the anterior temporal lobe with ventral and medial prefrontal cortices (21–24) implicated in anxiety (15). This fiber bundle shows a protracted developmental trajectory, with continuing development well into young adulthood (25, 26). We measured fractional anisotropy (FA), an index of connectivity derived from diffusion tensor imaging, and controlled for sex, ancestry, and site (i.e., imaging facility at which the scan occurred). A significant linear effect of age [$F(1,1,031) = 305.985$; $P < 2.2 \times 10^{16}$] on FA was observed in the UF (Fig. S1). Consistent with our earlier results of enhanced adult frontoamygdala connectivity as a function of the FAAH A385 allele (14), there was a main effect of the FAAH genotype on UF FA [$F(1,1,031) = 17.858$; $P = 2.59 \times 10^{-5}$]. Moreover, consistent with our hypothesis, there was an age by genotype interaction [age × genotype interaction: $F(1,1,031) = 5.893$; $P = 0.0154$] (Fig. 2*A*), with the genotype effect apparent after 12 y of age [$F(1,491) = 14.02$; $P = 0.0002$; trend toward dose dependence association) (Fig. S2) but not before [$F(1,523) = 0.513$; $P = 0.474$]. Specificity of the FAAH genotypic effects on frontolimbic circuitry was shown using the corticospinal tract as a control, which showed a similar main effect of age [$F(1,1,031) = 531.616$; $P = 2.0 \times 10^{-16}$] but no effect of genotype [$F(1,1,031) = 2.699$; $P = 0.101$] or age by genotype interaction [$F(1,1,031) = 0.009$; $P = 0.927$] (Fig. S3). The age by genotype interaction on UF FA was significant, even when controlling for corticospinal FA [$F(1,1,030) = 6.532$; $P = 0.011$].

We have proposed that knock-in mice that recapitulate common human polymorphisms facilitate controlled experiments on an inbred genetic background and provide a valuable source of validation of human candidate gene associations (19). Therefore, we performed connectivity analyses in FAAH A385 allele knock-in mice ($FAAH^{A/A}$) and WT littermate controls ($FAAH^{C/C}$). Given previous findings of FAAH C385A effects on descending infralimbic (IL) to basolateral amygdala (BLA) projections but not ascending BLA to IL projections (14), we focused on IL to BLA projections. The anterograde tracer phaseolus vulgaris leucoagglutinin (PHA-L) was injected into the IL prefrontal cortex of mice to label axonal projections from IL to BLA as a measure of frontoamygdala connectivity (27). Connectivity analyses were performed as a function of age in $FAAH^{C/C}$ and $FAAH^{A/A}$ mice after PHA-L injections at P23, P45, and P75 corresponding to preadolescence, adolescence, and adulthood, respectively ($n = 7$ per genotype per age), by quantifying fiber density in the BLA. Consistent with the human findings, the tract tracing experiment revealed a significant age group by genotype interaction [$F(2,36) = 58.72$; $P < 0.0001$] on fiber density in the BLA (Fig. 2*B*). Posthoc Student's $t$ tests between genotypes within each age group showed enhanced projections from IL to BLA in adolescent [$t(12) = 13.81$; $P < 0.0001$] and adult [$t(12) = 12.49$; $P < 0.0001$] $FAAH^{A/A}$ mice relative to $FAAH^{C/C}$ mice but no differences in fiber density in preadolescent mice [$t(12) = 0.56$; $P = 0.583$] as a function of FAAH C385A genotype.

**FAAH A385 Allele Is Associated with Lower Anxiety in Adolescence but Not in Childhood Across Humans and Mice.** Prior studies have shown that anxiety disorders peak during adolescence (1, 2) when there are dynamic changes in AEA levels (10, 11) that impact anxiety-related frontolimbic circuitry (28–31). Moreover, we have shown that the FAAH A385 allele is associated with increased frontolimbic connectivity and lower anxiety in both mice and humans in adulthood (14). Based on this culmination of findings and our imaging results showing phenotypic differences in frontolimbic circuitry that emerge during adolescence, we hypothesized that there would be a similar age by genotype interaction on anxiety, with FAAH A385 allele carriers showing less anxiety during adolescence than noncarriers and no phenotypic differences during childhood. We tested this hypothesis in a subset of the PING Study participants with self-reported anxiety symptoms ($n = 214$) using our imaging results and participant mean age of 12 y old to determine a priori age group boundaries for childhood (less than 12 y of age) and adolescence (12 y of age and older). We show an age group by genotype interaction for anxiety controlling for sex, ancestry, and site [$F(1,198) = 6.23$; $P = 0.0134$] (Fig. 3*A*). Posthoc analyses controlling for age, sex, ancestry, and site within each age group showed that adolescent FAAH A385 allele carriers had lower self-reported anxiety than noncarriers [$F(1,102) = 8.96$; $P = 0.003$], a phenotypic pattern that did not reach significance in children [$F(1,83) = 3.82$; $P = 0.054$].

To constrain our interpretation of our human findings and control for genetic and environmental background differences, we tested anxiety-like behavior in $FAAH^{C/C}$ and $FAAH^{A/A}$ mice using the elevated plus maze (EPM) at P23, P45, and P65–P75. Consistent with the human findings, the EPM test showed a significant age group by genotype interaction on anxiety-like behavior [$F(1,45) = 4.922$; $P = 0.0316$] as measured by percentage of time in the open arms (Fig. 3*B*). Posthoc $t$ tests revealed that $FAAH^{A/A}$ mice spent more time in the open arms than $FAAH^{C/C}$ mice during adolescence [$t(15) = 2.49$; $P = 0.0261$] and adulthood [$t(15) = 2.45$; $P = 0.0326$) but not during preadolescence [$t(15) = 0.932$; $P = 0.3687$]. There was no FAAH C385A genotype by age group interaction effect on total distance traveled in the EPM, a nonanxiety-related behavior (Fig. S4).

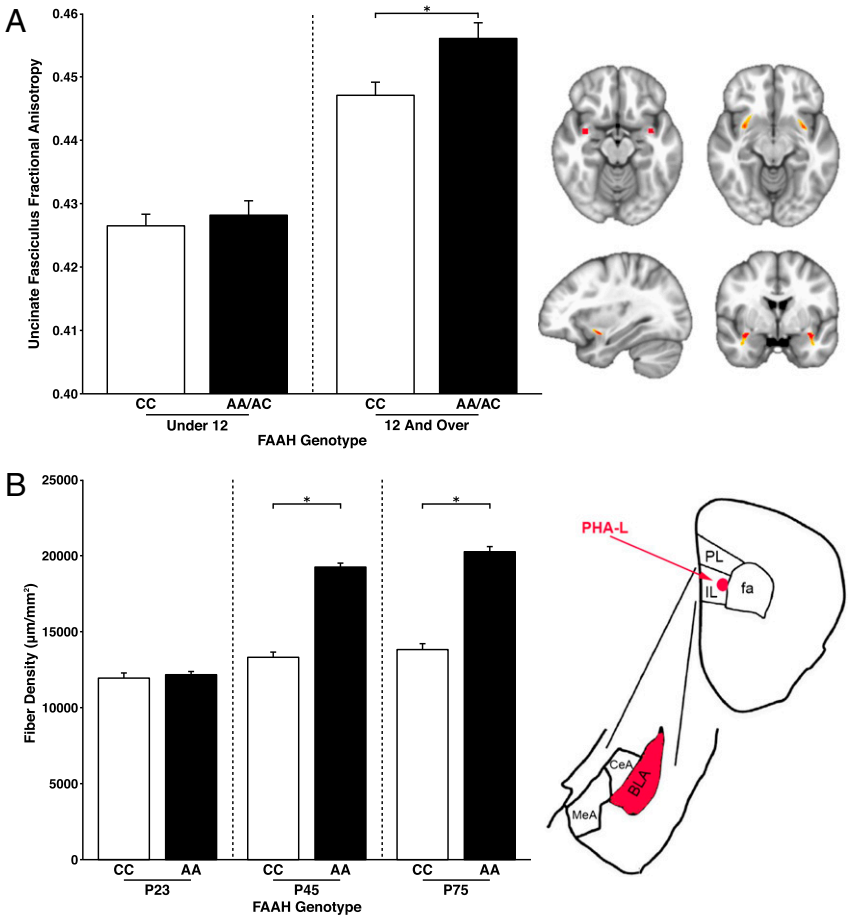


**Fig. 2.** Phenotypic differences in frontolimbic circuitry resulting from FAAH polymorphism emerge during adolescence in human and mouse. (*A*, *Left*) Posthoc analyses revealed a significant genotypic effect on UF FA in participants 12 y of age and older [$n = 509$; 249 females; $F(1,491) = 14.02$; $P = 0.0002$] but not in those under 12 y of age [$n = 541$; 259 females; $F(1,523) = 0.513$; $P = 0.474$]. (*A*, *Right*) Mask in Montreal Neurological Institute standard space where UF ascends from the temporal lobe used as the seed region for probabilistic tractography in humans (upper left); UF tract mask is derived from probabilistic tractography averaged across human participants ($n = 1,050$). (*B*, *Left*) Consistent with the findings in humans, a significant genotype by age group interaction [$F(2,36) = 58.72$; $P < 0.0001$] in IL afferent fibers to BLA emerged, such that knock-in mice (AA: $n = 7$ per age) had higher fiber density than WT mice (CC: $n = 7$ per age) during adolescence at age P45 ($P < 0.0001$) and adulthood at P75 ($P < 0.0001$). (*B*, *Right*) Drawing of anatomical boundaries and anterograde tracer targeted to IL and labeling afferents in BLA. CeA, central amygdala; MeA, medial amygdala; PL, prelimbic; *$P < 0.05$.

## Discussion

This developmentally informed translational approach with parallel studies in mice and humans provides converging evidence that effects of the FAAH C385A polymorphism on frontolimbic circuitry emerge during adolescence. $FAAH^{A/A}$ knock-in mice and human FAAH A385 allele carriers show stronger frontolimbic connectivity beginning in adolescence and extending into young adulthood but not in childhood. Consistent with stronger structural connectivity, adolescents but not younger mice or humans with the FAAH A385 allele showed lower anxiety, further suggesting developmental specificity in the phenotypic effects of the FAAH C385A polymorphism. This previously unidentified gene by development interaction may elucidate mechanisms underlying risk for anxiety disorders and suggest an important step toward precision medicine approaches that tailor treatment based on genetic variation and developmental stage (e.g., adolescence).

The adolescent emergence of FAAH C385A effects on frontolimbic circuitry in mice and humans suggests that normative developmental processes moderate the effects of the FAAH C385A polymorphism on frontolimbic development. CB1 expression, FAAH activity, and AEA levels are relatively stable during childhood but fluctuate dynamically across adolescence (10, 11, 32, 33). During this period of fluctuation, the developing system may be especially sensitive to differential expression of FAAH and consequently, AEA levels associated with the variant allele, especially as AEA levels wane. Specifically, as AEA levels decrease during midadolescence, additional quantitative effects of the FAAH A385 allele may increase. The moderation of phenotypic differences by developmental stage was not evident for a control tract, suggesting some specificity of the phenotypic effects to frontolimbic circuit development.

Consistent with the developmental emergence of FAAH C385A effects on frontolimbic connectivity, the effects of the FAAH A385 allele on anxiety also emerged during adolescence. Developmental alterations in the activity of FAAH and consequently, the levels of AEA in the system, may influence the development of neural circuitry and the emergence of anxiety (4). The endocannabinoid system has been associated with anxiety (34, 35), and we have shown that the FAAH A385 variant allele strengthens frontolimbic circuitry, enhances fear extinction, and decreases anxiety-like behaviors in mice and humans during adulthood (14). Effects of the FAAH C385A polymorphism on frontolimbic circuitry implicated in anxiety (15–18) are a likely mechanism underlying phenotypic differences in anxiety associated with the A385 allele. Specifically, functional effects of the A385 allele may enhance prefrontal regulation of the amygdala during fear (6, 7) through stronger frontoamygdala connectivity (14). In addition to revealing their developmental trajectory, here we extend these findings to structural connectivity in humans. Our prior work suggests that phenotypic differences resulting from the FAAH C385A polymorphism are specific to top-down connections from the IL to BLA, which were not apparent for the BLA to IL or the connections between the BLA and prelimbic cortex (14). Thus, greater regulation by top-down control of the amygdala may mediate the gain of function that FAAH A385 allele carriers exhibit in the domain of anxiety. Given the smaller sample of participants with anxiety scores in this study and the substantial effects of age on frontolimbic connectivity over this age range, it was not possible to uncouple these effects in a mediation model.

Despite the need for identification of differential genetic effects across development to inform risk and treatment of psychiatric disorders, gene by development interactions have remained largely elusive. Moreover, the challenges of mapping psychiatric disorders onto neurobiology, including nonreplication of past candidate gene studies, has hindered progress in clinical practice. Conducting parallel studies across species allows for

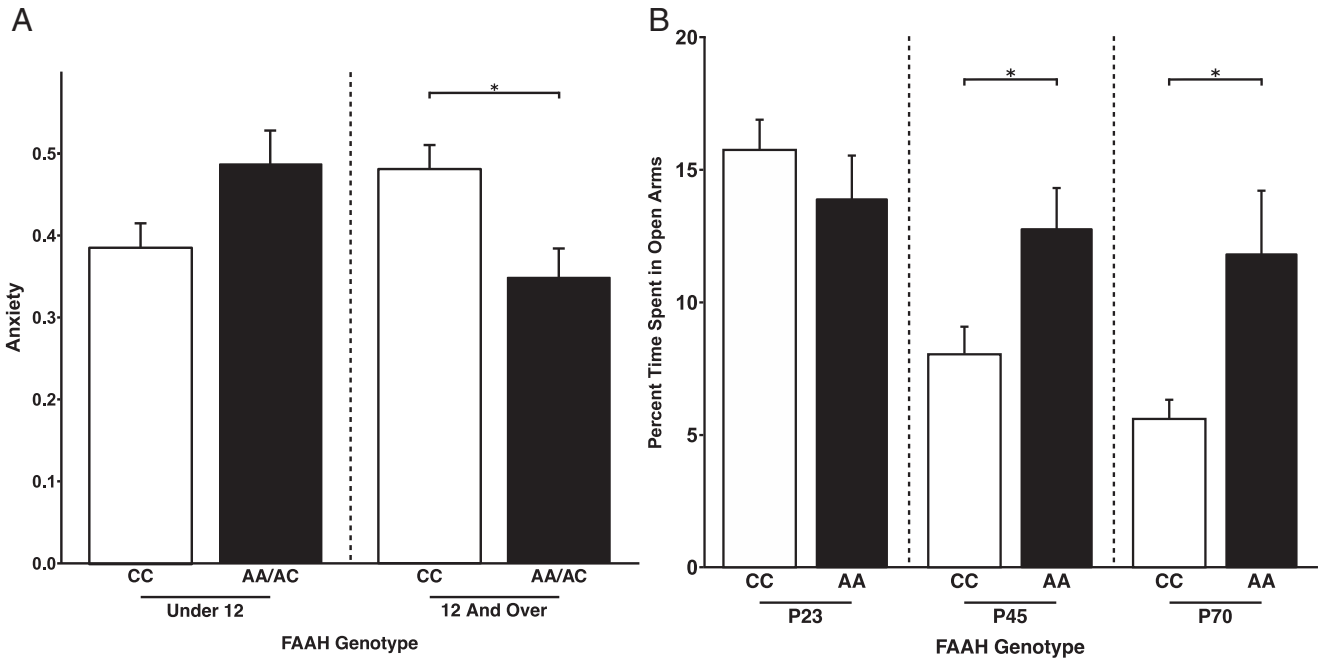


**Fig. 3.** Phenotypic differences in anxiety resulting from FAAH polymorphism emerge during adolescence in human and mouse. (*A*) A significant gene by development interaction [$F(1,198) = 6.2269$; $P = 0.0134$] on anxiety revealed that A allele carriers ($n = 54$; 19 females) had lower anxiety than C homozygotes ($n = 63$; 30 females) during adolescence [$F(1,102) = 8.96$; $P = 0.00346$] but not during childhood [$F(1,83) = 3.82$; $P = 0.054$; A allele carriers: $n = 32$; 21 females; C homozygotes: $n = 65$; 28 females]. These findings parallel the adolescent emergence of stronger frontolimbic connectivity among A allele carriers. (*B*) Consistent with the finding in humans, a significant genotype by age group interaction [$F(1,45) = 4.922$; $P = 0.0316$] revealed that $FAAH^{A/A}$ mice (P23: $n = 9$; P45: $n = 9$; P65–P75: $n = 10$) showed less anxiety-like behavior than $FAAH^{C/C}$ mice (P23: $n = 6$; P45: $n = 8$; P65–P75: $n = 7$) during adolescence and adulthood, but not during childhood, as measured by percentage of time spent in the open arms of the EPM. $^*P < 0.05$.

greater control of environmental and genetic background (e.g., in rodents) while enabling rapid translational discovery by leveraging conserved elements of neural and behavioral systems to identify genotype–phenotype relationships (19, 36–38). By integrating a developmentally informed approach with parallel rodent and human studies (Fig. 4), we have established convergence and cross-species validation of the developmental emergence of FAAH C385A effects on frontolimbic circuitry. Ultimately, such translational studies can facilitate scientific consensus that will permit the implementation of developmental biomarkers guiding clinical practice.

The finding that FAAH C385A effects on frontolimbic circuitry and anxiety emerge during adolescence may prove valuable in enhancing personalized medicine for anxiety disorders, which are the most common psychiatric disorders during adolescence. Despite dynamic changes across brain development, many treatments are based on principles studied in adults; delineating the biological state of the developing brain is critical for optimizing treatment for children and adolescents (3). Tailoring clinical practice based on developmental stage and individual genotypic differences may indicate which treatments will be most effective for which patients. Although any single common polymorphism is unlikely to be sufficient for personalizing treatments, this work may contribute to efforts to target treatments that rely on endocannabinoid signaling (e.g., FAAH inhibitors). Most recently, the role of endocannabinoids in treatment with selective serotonin reuptake inhibitors has been elucidated, suggesting additional implications for use of selective serotonin reuptake inhibitors or their combination with exposure-based therapies. Specifically, BLA-specific CB1 receptors and fluoxetine-induced increases in AEA mediated the effects of fluoxetine (but not citalopram) on fear extinction (39). Given the high incidence of anxiety disorders during adolescence (1) and prior evidence of diminished fear extinction during adolescence across species (40–42), these findings in the context of recent work on treatment mechanisms related to the endocannabinoid system have significant potential to optimize treatment for anxiety during this sensitive window of development.

## Conclusions

A developmentally informed approach integrating multiple levels of analysis across parallel studies in humans and mice engineered to recapitulate common human polymorphisms can identify reliable and precise genotype–phenotype relationships. In this report, we have shown that the effects of FAAH C385A genotype on frontolimbic connectivity vary as a function of developmental stage, emerging in early adolescence when endocannabinoid signaling is decreasing. This developmental trajectory coincides with the onset of anxiety disorders in many individuals and may contribute to interindividual variation in anxiety disorders and their treatment during adolescence and beyond. Our results underscore the importance of considering normative developmental neurobiology in characterizing the phenotypic effects of common human polymorphisms and their association with atypical development. Moreover, these findings highlight how phenotypic expression of common polymorphisms varies as a function of developmental changes in gene expression and neural circuit maturation and have broad implications for the development of common polymorphisms as potential biomarkers guiding psychiatric care.

## Methods

**Human Participants.** Data used for this study were obtained from the PING Study database (pingstudy.ucsd.edu) (*SI Methods*) (20). Participants included an initial sample of 1,221 typically developing individuals ranging in age from 3 to 21 y old who had diffusion scans collected in the multisite PING Study. Details on the recruitment, ascertainment, behavioral, genetic, and neuroimaging methods and acquisition in the PING Study are summarized below (details are in refs. 43–46). All participants provided informed consent (age 18 y old and older) or parental informed consent with child assent (ages 7–17 y old) in accordance with policies of the Institutional Review Boards of the sites of participation. Compensation was provided as agreed on during the consent process. In total, 1,050 individuals (mean age = 12.11 y old; SD = 4.80; range = 3.0–21.0; 518 females) (Table S1) from the PING Study database were included in this work after 171 participants from the initial

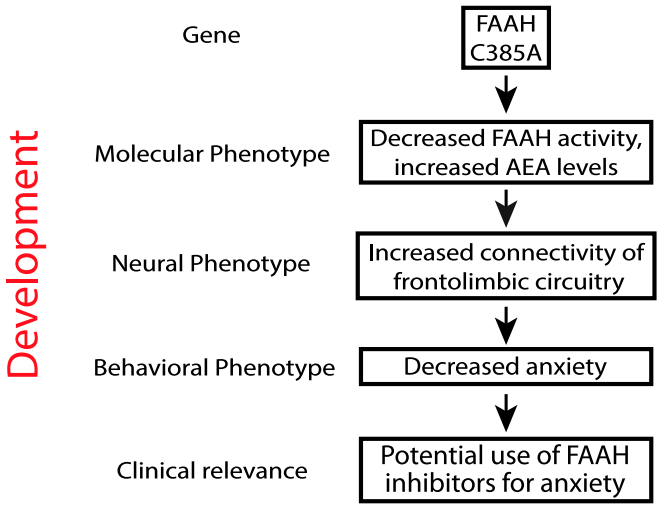


**Fig. 4.** Developmentally informed vertically integrated translational approach to genetic variation and treatment targets across development. We have used developmentally informed parallel human and mouse studies to identify the relevance and impact of the FAAH C385A polymorphism on brain biochemistry, neurocircuitry, behavior, and symptoms (i.e., vertical integration across multiple levels of analysis) during development and identified a previously unidentified gene by development interaction.

sample were excluded for excessive movement during image acquisition ($n$ = 2) or insufficient information for age, sex, ancestry, or genotype ($n$ = 169).

**Diffusion Imaging Data Preprocessing and FA Analysis.** Diffusion MRI data were obtained from the PING Study database. Acquisition protocols for a high-resolution, T1-weighted scan and diffusion-weighted scans were standardized across sites dependent on the make of scanner, with most parameters constant across all locations (*SI Methods*). Image preprocessing and analysis were performed with a customized processing pipeline using Analysis of Functional NeuroImages (47) and FMRIB Software Library software packages (48). Images were corrected for both susceptibility-induced and eddy current distortions (49). Participant head movement during image acquisition was calculated, and realignment was performed across gradient direction slices. Gradient vector directions were rotated based on the motion correction. Gradient slices that were found to have head displacement greater than one-half of a voxel (1.25 mm) were excluded from the diffusion directions used for additional analyses, because data for that gradient direction were likely inaccurate because of movement. If more than one-half of the gradient slices in a participant's data exceeded the movement threshold of 1.25 mm, the participant was excluded from additional analysis.

We examined structural connectivity for an a priori tract of interest, the UF, based on its identification as a major white matter tract connecting the prefrontal cortex and amygdala (22) and our prior evidence of phenotypic differences across mice and humans in frontoamygdala connectivity (14). Probabilistic tractography was used to determine UF masks on a participant by participant basis. Diffusion data were modeled using a crossing fiber technique described previously (Bayesian estimation of diffusion parameters obtained using sampling techniques) (50). A two-fiber model was created to perform probabilistic tractography and FA analysis. To determine the location of the UF in each participant, a mask in standard Montreal Neurological Institute (MNI) space was created to use as a seed region for tractography. The seed was placed at the site where the UF is known to ascend from the temporal lobe and loop anteriorly into the frontal lobe (Fig. 2*A*). An exclusionary mask was also placed posteriorly to the seed region to prevent detection of any tracts traveling posteriorly from the seed.

Participant FA maps were transformed into MNI space using a standard FA map, and probabilistic tractography was performed using the seed described. This technique resulted in individualized probabilistic maps, where the highly connected voxels showed a clear UF-shaped pattern that was easily isolated with a single threshold (4,000) held constant for all participants (Fig. 2*A*). The resulting probabilistic UF masks (both hemispheres) for each participant were inspected visually to ensure a trajectory consistent with the known shape of this major white matter tract (51). Each participant's FA map was then masked using individualized UF masks. The FA values of included voxels were averaged, resulting in an average UF FA value for each participant. To test the specificity for results of analyses of the UF, analyses were also performed on the corticospinal tract, which served as a control tract (*SI Methods* and Fig. S3).

**Human Genotyping.** The FAAH genotype was acquired by the PING Genomics Core by genome-wide genotyping on extracted DNA from saliva samples using the Illumina Human 660W-Quad Beadchip with markers passing quality control filters (sample cell rate >98%; SNP call rate >95%; minor allele frequency >5%). To assess ancestry and admixture proportions, a supervised clustering approach was implemented in the ADMIXTURE software (52), which clustered participant data into six clusters corresponding to six major continental populations: African, Central Asian, East Asian, European, Native American, and Oceanic.

**Anxiety Self-Report.** A subset of child and adolescent participants in the PING Study sample provided self-report on the Screen for Child Anxiety-Related Emotional Disorders (53). All child and adolescent participants who had genotype and self-reported anxiety ($n$ = 217; mean =12.69 y old; SD = 2.8; range =7.25–17.92; 100 females) were examined in the analyses of anxiety; three of these participants were excluded because of extreme scores on the anxiety measures (outliers <1.5× or >1.5× interquartile range), resulting in a total sample of 214 (Table S2).

**Mouse Model and Anterograde Tract Tracing Analyses.** We have previously validated a knock-in mouse model of FAAH C385A; generation of FAAH C385A mice is detailed in our prior work (14). WT mice express the human ancestral C385 allele, and replacement with the variant A385 allele resulted in knock-in mice having lower levels of FAAH protein and higher levels of AEA than WT mice. The FAAH knock-in mice were backcrossed >10 generations onto C57B16 mice (Charles River Laboratories). Only male mice were used for all experiments. All animals were kept on a 12:12-h light–dark cycle at 18 °C to 22 °C with food and water available ad libitum. Five mice were housed together per cage. All procedures were in accordance with the NIH *Guide for the Care and Use of Laboratory Animals* (54) and approved by the Institutional Animal Care and Use Committee of Weill Cornell Medical College.

Based on our a priori hypothesis about genotypic effects on the development of frontoamygdala circuitry, we used anterograde tracers in our FAAH knock-in mouse model to examine connectivity with the IL. Mice were microinjected with 20 nL of PHA-L [2.5% solution (wt/vol) in 0.05 M Tris-buffered saline (TBS) at pH 7.4; catalog no. AS-2300; Vector Laboratories] into the IL at P23, P45, and P75 to assess its projections to BLA (Fig. 2*B* and Table S3). After a survival time of 10 d after PHA-L injections, animals were deeply anesthetized with Euthasol (0.1 mL/10 g body weight) and perfused through the heart with 30 mL 0.9% saline followed by 120 mL 4% (wt/vol) paraformaldehyde in a 0.1 M phosphate buffer. Brains were removed and postfixed with 4% (wt/vol) paraformaldehyde in a 0.1 M phosphate buffer at 4 °C overnight and then, transferred to a sucrose solution (30% sucrose in 0.1 M phosphate buffer at 4 °C for 48 h). Coronal sections were cut on a freezing microtome (40 μm). Free-floating serial sections (take one out of every three) were washed (three times for 10 min each) in TBS and incubated for 30 min in a blocking solution containing 4% normal donkey serum and 1% BSA in TBS with 0.2% Triton X-100. Sections then were transferred in rabbit anti–PHA-L primary antibody (1:1,000; Vector Laboratories) diluted in the blocking solution mentioned above and incubated 24 h at 4 °C. Sections were incubated for 2 h with Alexa Fluor-labeled donkey anti-rabbit 555 (1:500; Invitrogen). Sections were mounted, coverslipped, and sealed with nail polish.

Injection sites were confirmed by referring to the Allen Mouse Brain Map (Allen Co.). Sections were observed under a Nikon 80i Fluorescent Microscope. Digital photography was performed using a MicroFire camera and FireFrame software (Optronics), and stereological estimation of cell density was performed using StereoInvestigator software (MicroBrightfield). Contours of the IL and BLA were drawn, and random sampling was applied to contours. Total volume of BLA was estimated using the Cavalieri method. Total cell numbers in IL were estimated using a fractionator, with counting frame size of 25 × 25 × 40 μm and sampling grid size of 100 × 100 μm. Detection of fiber density in BLA was performed using a stereological method. Briefly, sections were traced under a 4× lens, and then, perimetrics probe analysis was done under a 40× lens. Counting frame was set to 25 × 25 μm, and radius of the Merz coherent test system was set to 5 μm. Total length of all sampling sites was automatically calculated. For each animal, fiber density is obtained from the sum of the lengths divided by the sum of the areas for all sections. There were no differences in injections across all genotypes and age groups (Fig. S5).

**EPM to Measure Anxiety-Like Behavior in Mice.** The EPM task was conducted as described previously (*SI Methods*) (55). All mice studies were blinded to the investigator with regard to genotype for both the tract tracing and behavior studies.

**Statistical Analyses.** Statistical analyses were performed within the R statistical software package, version 2.15.1 (R Core Team). For human analyses, ANOVA

was conducted to examine the effects of age group (under 12 y old versus 12 y old and older) and FAAH genotype [homozygous CC vs. A allele carriers (AA, AC)] on FA while controlling for sex, ancestry, and site. When a significant age group by genotype interaction was detected, posthoc general linear model (GLM) analyses examined the effect of genotype within each age group in children (under 12 y old) as well as adolescents and young adults (12 y old and older) controlling for age (continuous given the wide age range), sex, ancestry, and site. Given a significant age group by genotype interaction on FA, we had an a priori hypothesis that genotype would have an effect on anxiety among adolescents and young adults (12 y old and older) but not among children (under 12 y old). This hypothesis was tested within each age group using a GLM controlling for age (continuous given the wide age range), sex, ancestry, and site. For mice analyses, ANOVA tested for an age group (P23, P45, or P75) by genotype (WT vs. knock in) interaction on fiber density and the percentage of time spent in the open arms during the EPM. For a significant age group by genotype effect, posthoc Student's *t* tests tested the effect of genotype within each age group. For humans, secondary exploratory analyses used a GLM to test for a dose-dependent effect of genotype on FA (AA > AC > CC) (Fig. S2) and anxiety (AA < AC < CC) (Fig. S6). Statistical tests were two-sided; values of $P < 0.05$ were considered statistically significant. Data are presented as means ± SEMs.

**ACKNOWLEDGMENTS.** This work was supported, in part, by the Samuel W. Perry III, MD Distinguished Award in Psychiatric Medicine (to D.G.G.); NIH Grants T32GM007739 (to the Weill Cornell/Rockefeller/Sloan Kettering Tri-Institutional MD/PhD Program, R.N.F., A.L., and A.T.D.), RC2DA029475 (to A.M.D., T.L.J., and B.J.C.), and U01DA041174 (to B.J.C.); a gift from the Mortimer D. Sackler, MD, family; a National Science Foundation Graduate Research Fellowship (to A.O.C.); and the New York-Presbyterian Youth Anxiety Center (F.S.L.).

1. Kessler RC, et al. (2005) Lifetime prevalence and age-of-onset distributions of DSM-IV disorders in the National Comorbidity Survey Replication. *Arch Gen Psychiatry* 62(6):593–602.
2. Paus T, Keshavan M, Giedd JN (2008) Why do many psychiatric disorders emerge during adolescence? *Nat Rev Neurosci* 9(12):947–957.
3. Lee FS, et al. (2014) Mental health. Adolescent mental health—opportunity and obligation. *Science* 346(6209):547–549.
4. Casey BJ, Glatt CE, Lee FS (2015) Treating the developing versus developed brain: Translating preclinical mouse and human studies. *Neuron* 86(6):1358–1368.
5. Hill MN, Patel S (2013) Translational evidence for the involvement of the endocannabinoid system in stress-related psychiatric illnesses. *Biol Mood Anxiety Disord* 3(1):19.
6. Hariri AR, et al. (2009) Divergent effects of genetic variation in endocannabinoid signaling on human threat- and reward-related brain function. *Biol Psychiatry* 66(1):9–16.
7. Gunduz-Cinar O, et al. (2013) Convergent translational evidence of a role for anandamide in amygdala-mediated fear extinction, threat processing and stress-reactivity. *Mol Psychiatry* 18(7):813–823.
8. Ellgren M, et al. (2008) Dynamic changes of the endogenous cannabinoid and opioid mesocorticolimbic systems during adolescence: THC effects. *Eur Neuropsychopharmacol* 18(11):826–834.
9. Heng L, Beverley JA, Steiner H, Tseng KY (2011) Differential developmental trajectories for CB1 cannabinoid receptor expression in limbic/associative and sensorimotor cortical areas. *Synapse* 65(4):278–286.
10. Lee TT, Hill MN, Hillard CJ, Gorzalka BB (2013) Temporal changes in N-acylethanolamine content and metabolism throughout the peri-adolescent period. *Synapse* 67(1):4–10.
11. Lee TT, Gorzalka BB (2012) Timing is everything: Evidence for a role of corticolimbic endocannabinoids in modulating hypothalamic-pituitary-adrenal axis activity across developmental periods. *Neuroscience* 204:17–30.
12. Lee TT, Hill MN, Lee FS (2016) Developmental regulation of fear learning and anxiety behavior by endocannabinoids. *Genes Brain Behav* 15(1):108–124.
13. Sipe JC, Chiang K, Gerber AL, Beutler E, Cravatt BF (2002) A missense mutation in human fatty acid amide hydrolase associated with problem drug use. *Proc Natl Acad Sci USA* 99(12):8394–8399.
14. Dincheva I, et al. (2015) FAAH genetic variation enhances fronto-amygdala function in mouse and human. *Nat Commun* 6:6395.
15. Kim MJ, Whalen PJ (2009) The structural integrity of an amygdala-prefrontal pathway predicts trait anxiety. *J Neurosci* 29(37):11614–11618.
16. Phan KL, et al. (2009) Preliminary evidence of white matter abnormality in the uncinate fasciculus in generalized social anxiety disorder. *Biol Psychiatry* 66(7):691–694.
17. Tromp DP, et al. (2012) Reduced structural connectivity of a major frontolimbic pathway in generalized anxiety disorder. *Arch Gen Psychiatry* 69(9):925–934.
18. Liao M, et al. (2014) White matter abnormalities in adolescents with generalized anxiety disorder: A diffusion tensor imaging study. *BMC Psychiatry* 14:41.
19. Glatt CE, Lee FS (2016) Common polymorphisms in the age of Research Domain Criteria (RDoC): Integration and translation. *Biol Psychiatry* 79(1):25–31.
20. Jernigan TL, et al. (2016) The Pediatric Imaging, Neurocognition, and Genetics (PING) Data Repository. *Neuroimage* 124(Pt B):1149–1154.
21. Ebeling U, von Cramon D (1992) Topography of the uncinate fascicle and adjacent temporal fiber tracts. *Acta Neurochir (Wien)* 115(3-4):143–148.
22. Ghashghaei HT, Barbas H (2002) Pathways for emotion: Interactions of prefrontal and anterior temporal pathways in the amygdala of the rhesus monkey. *Neuroscience* 115(4):1261–1279.
23. Croxson PL, et al. (2005) Quantitative investigation of connections of the prefrontal cortex in the human and macaque using probabilistic diffusion tractography. *J Neurosci* 25(39):8854–8866.
24. Johansen-Berg H, et al. (2008) Anatomical connectivity of the subgenual cingulate region targeted with deep brain stimulation for treatment-resistant depression. *Cereb Cortex* 18(6):1374–1383.
25. Lebel C, et al. (2012) Diffusion tensor imaging of white matter tract evolution over the lifespan. *Neuroimage* 60(1):340–352.
26. Von Der Heide RJ, Skipper LM, Klobusicky E, Olson IR (2013) Dissecting the uncinate fasciculus: Disorders, controversies and a hypothesis. *Brain* 136(Pt 6):1692–1707.
27. Gerfen CR, Sawchenko PE (1984) An anterograde neuroanatomical tracing method that shows the detailed morphology of neurons, their axons and terminals: Immunohistochemical localization of an axonally transported plant lectin, Phaseolus vulgaris leucoagglutinin (PHA-L). *Brain Res* 290(2):219–238.
28. Eluvathingal TJ, Hasan KM, Kramer L, Fletcher JM, Ewing-Cobbs L (2007) Quantitative diffusion tensor tractography of association and projection fibers in normally developing children and adolescents. *Cereb Cortex* 17(12):2760–2768.
29. Hasan KM, et al. (2009) Development and aging of the healthy human brain uncinate fasciculus across the lifespan using diffusion tensor tractography. *Brain Res* 1276:67–76.
30. Swartz JR, Carrasco M, Wiggins JL, Thomason ME, Monk CS (2014) Age-related changes in the structure and function of prefrontal cortex-amygdala circuitry in children and adolescents: A multi-modal imaging approach. *Neuroimage* 86:212–220.
31. Simmonds DJ, Hallquist MN, Asato M, Luna B (2014) Developmental stages and sex differences of white matter and behavioral development through adolescence: A longitudinal diffusion tensor imaging (DTI) study. *Neuroimage* 92:356–368.
32. Rodríguez de Fonseca F, Ramos JA, Bonnin A, Fernández-Ruiz JJ (1993) Presence of cannabinoid binding sites in the brain from early postnatal ages. *Neuroreport* 4(2):135–138.
33. Long LE, Lind J, Webster M, Weickert CS (2012) Developmental trajectory of the endocannabinoid system in human dorsolateral prefrontal cortex. *BMC Neurosci* 13:87.
34. Kathuria S, et al. (2003) Modulation of anxiety through blockade of anandamide hydrolysis. *Nat Med* 9(1):76–81.
35. Chhatwal JP, Davis M, Maguschak KA, Ressler KJ (2005) Enhancing cannabinoid neurotransmission augments the extinction of conditioned fear. *Neuropsychopharmacology* 30(3):516–524.
36. Feyder M, et al. (2010) Association of mouse Dlg4 (PSD-95) gene deletion and human DLG4 gene variation with phenotypes relevant to autism spectrum disorders and Williams' syndrome. *Am J Psychiatry* 167(12):1508–1517.
37. Andero R, et al. (2013) Amygdala-dependent fear is regulated by Oprl1 in mice and humans with PTSD. *Sci Transl Med* 5(188):188ra73.
38. Qiu S, Aldinger KA, Levitt P (2012) Modeling of autism genetic variations in mice: Focusing on synaptic and microcircuit dysfunctions. *Dev Neurosci* 34(2-3):88–100.
39. Gunduz-Cinar O, et al. (October 30, 2015) Fluoxetine facilitates fear extinction through amygdala endocannabinoids. *Neuropsychopharmacology*, 10.1038/npp.2015.318.
40. Pattwell SS, et al. (2012) Altered fear learning across development in both mouse and human. *Proc Natl Acad Sci USA* 109(40):16318–16323.
41. McCallum J, Kim JH, Richardson R (2010) Impaired extinction retention in adolescent rats: Effects of D-cycloserine. *Neuropsychopharmacology* 35(10):2134–2142.
42. Drysdale AT, et al. (2014) Fear and anxiety from principle to practice: Implications for when to treat youth with anxiety disorders. *Biol Psychiatry* 75(11):e19–e20.
43. Brown TT, et al. (2012) Neuroanatomical assessment of biological maturity. *Curr Biol* 22(18):1693–1698.
44. Fjell AM, et al.; Pediatric Imaging, Neurocognition, and Genetics Study (2012) Multimodal imaging of the self-regulating developing brain. *Proc Natl Acad Sci USA* 109(48):19620–19625.
45. Walhovd KB, et al.; Pediatric Imaging, Neurocognition, and Genetics Study (2012) Long-term influence of normal variation in neonatal characteristics on human brain development. *Proc Natl Acad Sci USA* 109(49):20089–20094.
46. Akshoomoff N, et al. (2014) The NIH Toolbox Cognition Battery: Results from a large normative developmental sample (PING). *Neuropsychology* 28(1):1–10.
47. Cox RW (1996) AFNI: Software for analysis and visualization of functional magnetic resonance neuroimages. *Comput Biomed Res* 29(3):162–173.
48. Smith SM, et al. (2004) Advances in functional and structural MR image analysis and implementation as FSL. *Neuroimage* 23(Suppl 1):S208–S219.
49. Andersson JLR, Skare S, Ashburner J (2003) How to correct susceptibility distortions in spin-echo echo-planar images: Application to diffusion tensor imaging. *Neuroimage* 20(2):870–888.
50. Behrens TEJ, Berg HJ, Jbabdi S, Rushworth MF, Woolrich MW (2007) Probabilistic diffusion tractography with multiple fibre orientations: What can we gain? *Neuroimage* 34(1):144–155.
51. Wakana S, Jiang H, Nagae-Poetscher LM, van Zijl PCM, Mori S (2004) Fiber tract-based atlas of human white matter anatomy. *Radiology* 230(1):77–87.
52. Alexander DH, Novembre J, Lange K (2009) Fast model-based estimation of ancestry in unrelated individuals. *Genome Res* 19(9):1655–1664.
53. Birmaher B, et al. (1997) The Screen for Child Anxiety Related Emotional Disorders (SCARED): Scale construction and psychometric characteristics. *J Am Acad Child Adolesc Psychiatry* 36(4):545–553.
54. National Research Council (US) Committee for the Update of the Guide for the Care and Use of Laboratory Animals (2011) *Guide for the Care and Use of Laboratory Animals* (National Academies Press, Washington, DC), 8th Ed.
55. Lister RG (1987) The use of a plus-maze to measure anxiety in the mouse. *Psychopharmacology (Berl)* 92(2):180–185.

# Supporting Information

## Gee et al. 10.1073/pnas.1600013113

### SI Methods

**PING Study.** The PING Study was launched in 2009 by the National Institute on Drug Abuse and the Eunice Kennedy Shriver National Institute of Child Health and Human Development as a 2-y project of the American Recovery and Reinvestment Act. The primary goal of the PING Study has been to create a data resource of highly standardized and carefully curated MRI data, comprehensive genotyping data, and developmental and neuropsychological assessments for a large cohort of developing individuals ages 3–21 y old. The scientific aim of the project is, by openly sharing these data, to amplify the power and productivity of investigations of healthy and disordered development in children and adolescents and increase understanding of the origins of variation in neurobehavioral phenotypes.

**MRI Protocols.** Four different scanners were used across the 10 PING Study sites. At each site, a high-resolution, T1-weighted scan was acquired for normalization of diffusion-weighted scans to a standard template. Two series of directional diffusion-weighted scans were collected at each site in interleaved, transverse, 2.5-mm slices using echoplanar imaging (240 × 240-mm in-plane resolution; 240-mm field of view; $b$ value = 1,000 s/mm$^2$). At the beginning of each sequence of directional scans, an additional scan at $b$ value = 0 was collected using identical parameters. To correct for known distortion introduced by phase-encoding direction in diffusion-weighted scans, two additional scans with $b$ value = 0 were collected. One scan used anterior to posterior phase encoding, whereas the other used posterior to anterior phase encoding. These additional scans were incorporated in additional preprocessing steps (*Methods*, *Diffusion Imaging Data Preprocessing and FA Analysis*). Acquisition parameters for the T1- and diffusion-weighted scans that were specific to each scanner are detailed below.

***Siemens MAGNETOM TrioTim (3.0-T) MRI Scanner (Siemens Medical Solutions).*** The high-resolution, T1-weighted scan was acquired in 160 1.2-mm slices (256 × 192-mm in-plane resolution; 256-mm field of view). For diffusion-weighted scans, two series of 30 directional scans were collected in 68 slices [repetition time (TR) = 19 s; echo time (TE) = 91 ms; anterior to posterior phase encoding].

***General Electric Discovery 750 3.0-T MRI Scanner (General Electric Company).*** The high-resolution, T1-weighted scan was acquired in 166 1.2-mm slices (256 × 192-mm in-plane resolution; 240-mm field of view). For diffusion-weighted scans, two series of 30 directional scans were collected in 51 slices (TR = 8 s; TE = 80.7 ms; right to left phase encoding).

***General Electric Sigma HDx (3.0-T) MRI Scanner (General Electric Company).*** The high-resolution, T1-weighted scan was acquired in 166 1.2-mm slices (256 × 192-mm in-plane resolution; 240-mm field of view). For diffusion-weighted scans, two series of 30 directional scans were collected in 51 slices (TR = 13.6 s; TE = 83 ms; right to left phase encoding).

***Phillips Achieva (3.0-T) MRI Scanner (General & Company).*** The high-resolution, T1-weighted scan was acquired in 170 1.2-mm slices (256 × 256-mm in-plane resolution; 240-mm field of view). For diffusion-weighted scans, two series of 32 directional scans were collected in 60 slices (TR = 9 s; TE = 91.14 ms; anterior to posterior phase encoding).

**Control Analysis: Corticospinal Tract.** The corticospinal tract was determined using probabilistic tractography, masking specifically for all tracts that traverse the lateral portions of the internal capsule posterior limbs. The mask was drawn based on the axial plane of MNI standard space ($z$ = 6) to cover the entire lateral posterior limbs. Participant FA maps were transformed into MNI space using a standard FA map, and probabilistic tractography was performed using the seed described. Resulting probabilistic corticospinal masks (both hemispheres; threshold value = 4,000) for each participant were inspected visually to ensure a trajectory consistent with the known shape of this white matter tract (51). Each participant's FA map was then masked using their individualized corticospinal tract mask (Fig. S3). The FA values of included voxels were averaged across hemispheres to calculate a final FA value for each participant for use in statistical analysis.

**EPM to Measure Anxiety-Like Behavior in Mice.** The maze was constructed of gray Plexiglas raised 70 cm above the floor and consisted of two opposite closed arms with 14-cm-high opaque walls and two opposite open arms of the same size (29 × 6 cm). All sessions were carried out under dim light, and all animals were habituated to the behavior room before their test sessions. The movements of the animals were captured by a digital camera from above and live-tracked using Ethovision 5.1 (Noldus). A single testing session of 10 min was carried out under dim light (~6 Lux in the center of maze). To begin a trial, the animal was placed in the center of the maze facing an open arm. Anxiety-like behavior was assessed by computing the percentage of time spent in the open arms out of 10 min. Between sessions, the maze was thoroughly cleaned with 70% ethanol to remove any residual odors. All behavioral sessions were conducted from 12:00 PM to 5:00 PM in the light phase of the cycle.

### PING Consortium

**Part A: Infrastructure.**

***Coordinating Core:***

Terry L. Jernigan, Ph.D., UC San Diego, Co-PI of PING, Core PI
Connor McCabe, B.S., UC San Diego

***Assessment Core:***

Linda Chang, M.D., U Hawaii, Co-PI of PING, Core PI
Natacha Akshoomoff, Ph.D., UC San Diego
Erik Newman, Ph.D., UC San Diego

***MRI Post-processing Core:***

Anders M. Dale, Ph.D., UC San Diego, Co-PI of PING, Core PI

***MRI Acquisition Core:***

Thomas Ernst, Ph.D., U Hawaii, Co-PI of PING, Core Co-PI
Anders M. Dale, Ph.D., UC San Diego, Core Co-PI
Peter Van Zijl, Ph.D., KKI
Joshua Kuperman, Ph.D., UC San Diego

***Genetics Core:***

Sarah Murray, Ph.D., Scripps Translational Science Institute, Co-PI of PING, Core PI
Cinnamon Bloss, Ph.D., Scripps Translational Science Institute
Nicholas J. Schork, Ph.D., Scripps Translational Science Institute

***Informatics and Biostatistics:***

Mark Appelbaum, Ph.D., UC San Diego
Anthony Gamst, Ph.D., UC San Diego
Wesley Thompson, Ph.D., UC San Diego
Hauke Bartsch, Ph.D., UC San Diego

**Part B: Investigators by Data Collection Site. (3 author maximum per site):**

***University of California, San Diego:***

Terry L. Jernigan, Ph.D.
Anders M. Dale, Ph.D.
Natacha Akshoomoff, Ph.D.

***University of Hawaii:***

Linda Chang, M.D.
Thomas Ernst, Ph.D.
Brian Keating, Ph.D.

***University of California, Davis:***

David Amaral, Ph.D.

***University of California, Los Angeles:***

Elizabeth Sowell, Ph.D.

***Kennedy Krieger Institute, Johns Hopkins University:***

Walter Kaufmann, M.D.
Peter Van Zijl, Ph.D.
Stewart Mostofsky, M.D.

***Sackler Institute, Weill Cornell Medical College:***

B.J. Casey, Ph.D.
Erika J. Ruberry, B.A.
Alisa Powers, B.A.

***Massachusetts General Hospital, Harvard University:***

Bruce Rosen, M.D., Ph.D.
Tal Kenet, Ph.D.

***University of Massachusetts:***

Jean Frazier, M.D.
David Kennedy, Ph.D.
Yale University:
Jeffrey Gruen, M.D.

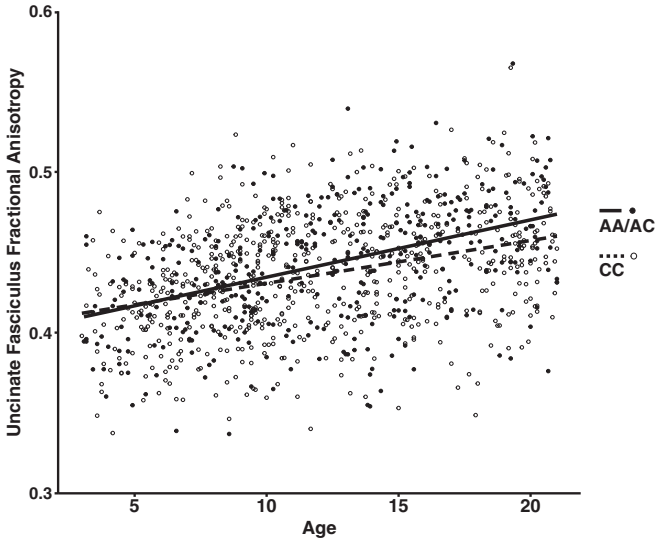


**Fig. S1.** FAAH genotype by age interaction for FA in the UF. FA of the UF showed a significant increase with age [$F(1,1,031) = 305.985$; $P < 2.2 \times 10^{16}$; plotted as a function of age in A allele carriers ($n = 420$; 208 females) and C homozygotes ($n = 630$; 310 females)]. A significant age by genotype interaction [age by genotype interaction: $F(1,1,031) = 5.893$; $P = 0.0154$] revealed that the main effect of genotype [$F(1,1,031) = 17.858$; $P = 2.59 \times 10^{-5}$] emerged during adolescence.

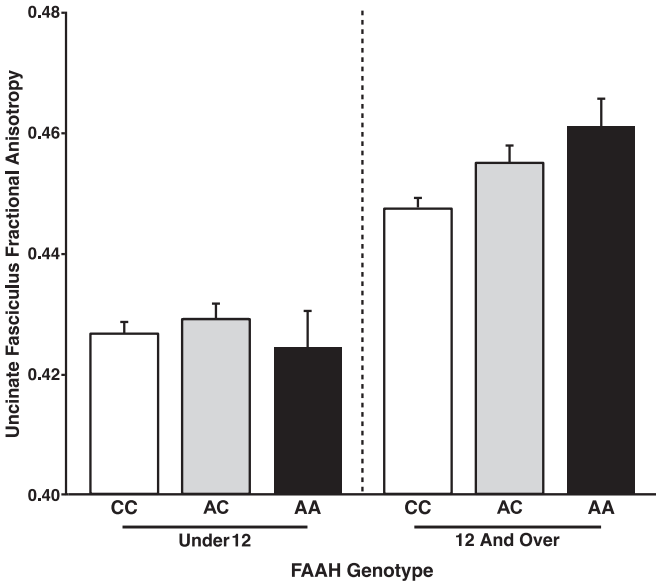


**Fig. S2.** Trend for dose dependence association between FAAH genotype and frontolimbic circuitry emerging during adolescence. There was a trend toward a linear effect of number of A alleles on UF FA among participants 12 y of age and older [$F(2,491) = 2.03$; $P = 0.154$; AA: $n = 41$; 15 females; AC: $n = 182$; 90 females; CC: $n = 286$; 144 females]. However, there was no effect of number of A alleles on UF FA among participants under 12 y of age [$F(2,523) = 1.92$; $P = 0.167$; AA: $n = 29$; 11 females; AC: $n = 168$; 92 females; CC: $n = 344$; 166 females]. Data are presented as means ± SEMs.

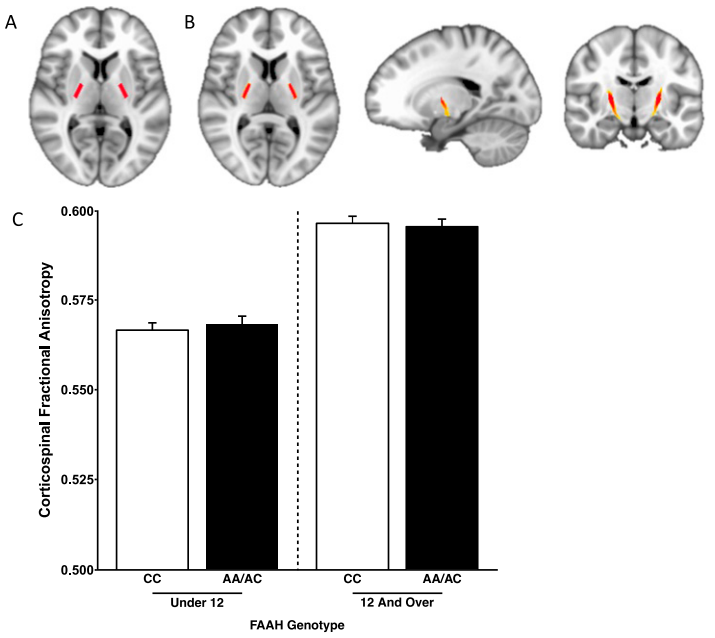


**Fig. S3.** No FAAH genotype by age group interaction for FA in the corticospinal tract. (*A*) Mask in Montreal Neurological Institute standard space of bilateral internal capsules to serve as the seed region for probabilistic tractography. (*B*) Corticospinal tract mask derived from probabilistic tractography averaged across human participants ($n = 1,050$). (*C*) There was a significant effect of age on FA in the corticospinal tract [$F(1,1,031) = 531.616$; $P = 2.0 \times 10^{-16}$]. However, there was no main effect of genotype [$F(1,1,031) = 2.699$; $P = 0.101$] or age by genotype interaction [$F(1,1,031) = 0.009$; $P = 0.927$], suggesting specificity of the developmental effects of the FAAH genotype on frontolimbic circuitry. Data are presented as means ± SEMs.

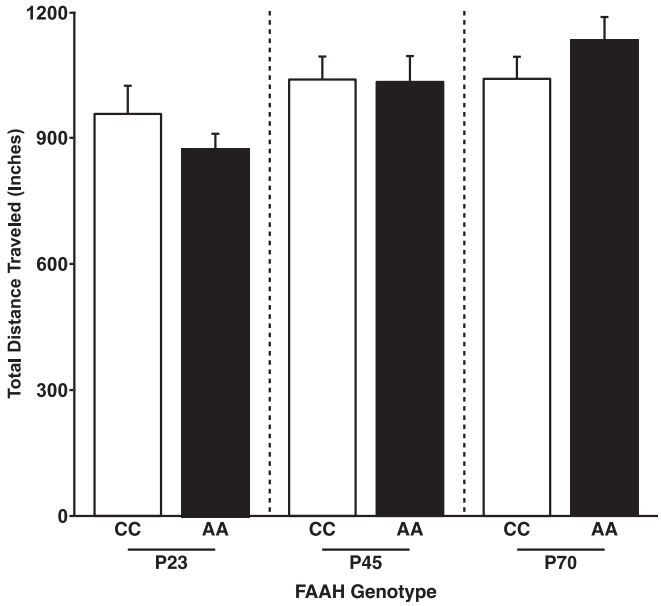


**Fig. S4.** No FAAH genotype by age group interaction for total distance traveled in the EPM. Despite a genotype by age group interaction for percentage of time spent in the open arms, there was no genotype by age group interaction for total distance traveled in the EPM [$F(1,45) = 2.59$; $P = 0.114$]. Data are presented as means ± SEMs.

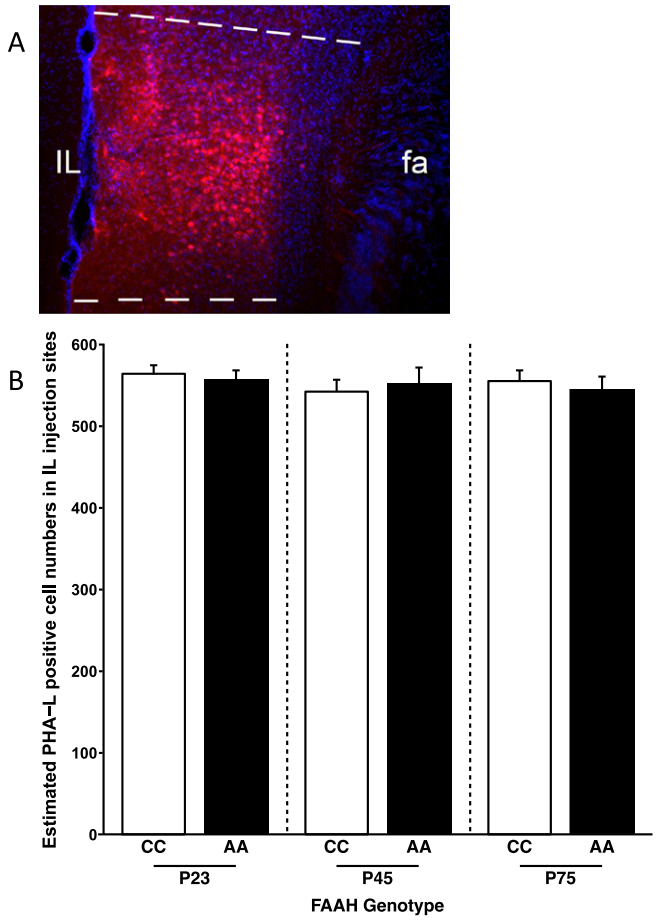


**Fig. S5.** PHA-L injections in IL cortex of mice. (*A*) Representative site of IL injection of PHA-L; PHA-L–like positive neurons and neuropil deposits are well-defined in IL, and PHA-L–like immunoreactive positive neurons (red) are counterstained with DAPI. This assessment of injection accuracy was carried out for all seven mice per genotype per age, and all of the injections were within the IL and did not overlap with neighboring regions, such as the prelimbic prefrontal cortex. (*B*) Bar graph showing numbers of PHA-L–positive cell bodies in IL in different genotypes and ages based on stereological estimation of cell density using the fractionator estimation method. There were no main effects of age [$F(1,36) = 0.0273$; $P = 0.789$] or genotype [$F(2,36) = 0.453$; $P = 0.639$] and no age by genotype interaction [$F(2,36) = 0.309$; $P = 0.736$]. Data are presented as means ± SEMs.

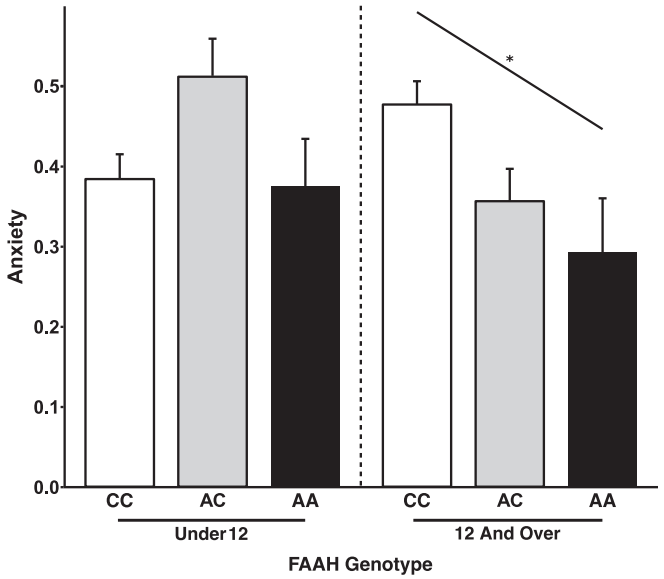


**Fig. S6.** Dose-dependent association between FAAH genotype and anxiety during adolescence. There was a linear effect of number of A alleles on anxiety among participants 12 y of age and older [$F(2,102) = 4.37$; $P = 0.031$; AA: $n = 10$; 4 females; AC: $n = 44$; 15 females; CC: $n = 63$; 30 females]. However, there was no linear effect of number of A alleles on anxiety among participants under 12 y of age [$F(2,83) = 0.554$; $P = 0.459$; AA: $n = 6$; 4 females; AC: $n = 26$; 17 females; CC: $n = 65$; 28 females]. Data are presented as means ± SEMs.

**Table S1. Diffusion tensor imaging sample ($n$ = 1,050): Demographic characteristics by genotype**

| | Under 12 y of age | | | 12 y of Age and older | | |
|---|---|---|---|---|---|---|
| Characteristics | CC | AC | AA | CC | AC | AA |
| *n* | 344 | 168 | 29 | 286 | 182 | 41 |
| Mean age, y (SD)* | 8.14 (2.27) | 8.01 (2.39) | 8.45 (2.53) | 16.51 (2.64) | 16.17 (2.55) | 16.22 (2.49) |
| Sex, female/male† | 166/178 | 92/76 | 11/18 | 144/142 | 90/92 | 15/26 |

*Age did not differ by genotype within the group under 12 y of age [$F(2,540) = 0.493$; $P = 0.611$] or 12 y of age and older [$F(2,508) = 1.023$; $P = 0.360$].
†Sex did not differ by genotype within the group under 12 y of age [$\chi^2(2) = 3.62$; $P = 0.164$] or 12 y of age or older [$\chi^2(2) = 2.75$; $P = 0.253$].

**Table S2. Anxiety subsample ($n$ = 214): Demographic characteristics and anxiety self-report by genotype**

| | Under 12 y of age | | | 12 y of Age and older | | |
|---|---|---|---|---|---|---|
| Characteristics | CC | AC | AA | CC | AC | AA |
| *n* | 65 | 26 | 6 | 63 | 44 | 10 |
| Mean age, y (SD)* | 10.0 (0.99) | 9.96 (0.85) | 9.50 (1.31) | 14.83 (1.46) | 14.79 (1.73) | 15.80 (1.79) |
| Sex, female/male† | 28/37 | 17/9 | 4/2 | 30/33 | 15/29 | 4/6 |
| Mean anxiety (SD) | 0.384 (0.25) | 0.512 (0.24) | 0.375 (0.15) | 0.479 (0.23) | 0.358 (0.27) | 0.294 (0.21) |

*Age did not differ by genotype within the group under 12 y of age [$F(2,96) = 0.722$; $P = 0.488$] or 12 y of age and older [$F(2,116) = 1.759$; $P = 0.177$].
†Sex did not differ by genotype within the group under 12 y of age [$\chi^2(2) = 4.36$; $P = 0.113$] or 12 y of age or older [$\chi^2(2) = 1.96$; $P = 0.375$].

**Table S3. Coordinates for IL injections**

| Age | AP (mm) | ML (mm) | DV (mm) |
|---|---|---|---|
| P23 | 1.60 | 0.35 | 2.30 |
| P45 | 1.70 | 0.40 | 2.50 |
| P75 | 1.70 | 0.40 | 2.50 |

AP, anterior–posterior; DV, dorsal–ventral; ML, medial–lateral.